Hypocotyl Development in Arabidopsis and other Brassicaceae Displays Evidence of Photoperiodic Memory

James Ronald[1], Sarah C.L Lock[1], Will Claydon[1], Zihao Zhu[2], Kayla McCarthy[1], Elizabeth Pendlington[1], Ethan J. Redmond[1], Gina Y.W. Vong[1], Sanoj P. Stanislas[1], Seth J. Davis[1], Marcel Quint[2], Daphne Ezer[1]*.

[1]Department of Biology, University of York, Wentworth Way, Heslington, York YO10 5DD, UK.
[2]Institute of Agricultural and Nutritional Sciences, Martin Luther University Halle-Wittenberg, Halle (Saale), Germany.

*Corresponding authors:
Daphne Ezer (daphne.ezer@york.ac.uk)

Abstract

Sensing and responding to photoperiod changes is essential for plants to adapt to seasonal progression. Most of our understanding of how plants sense photoperiodic changes is through studies on flowering time [1]. However, other aspects of plant development are regulated by the photoperiod, including hypocotyl elongation [2, 3]. Unlike flowering, hypocotyl elongation displays a greater plasticity to changes in the photoperiod with increases in daylength causing greater inhibition of growth until a threshold is met [3]. Although we have a good understanding of how the photoperiod regulates hypocotyl elongation [2, 3], previous investigations have only looked at hypocotyl development under a constant photoperiod. It is unknown if changes in the photoperiod during development influence hypocotyl elongation and whether the initial photoperiod exposure continues to impact subsequent development. Here, we developed a physiological assay to investigate this question. We have discovered that hypocotyl elongation is influenced by a memory of past photoperiod exposure in Arabidopsis and Brassicaceae cultivars used for microgreen agriculture. Photoperiodic memory persisted for multiple days, although it weakened over time, and the strength of the memory was dependent on the genetic background. We identified that phyB and ELF3, key regulators of hypocotyl development [4, 5], were required for photoperiodic memory. Finally, we identified that the circadian clock is unlikely to function as a repository for photoperiodic memory as circadian rhythms quickly re-aligned with the new photoperiod. In summary, our work highlights for the first-time evidence of a photoperiodic memory that can control plant development.

Results and Discussion

Designing a photoperiodic memory experimental assay

To understand whether hypocotyl development in *Arabidopsis thaliana* (Arabidopsis hereafter) is influenced by prior exposure to a given different photoperiod (Figure 1A) we designed the following assay. Here, stratified seeds were firstly germinated under constant white light for 24 hours to synchronize germination before seedlings were then provided two days of photoperiodic information, either short-days (8/16 light/dark) or long-days (16/8 light/dark). On day 3, seedlings were then either transferred to the reciprocal photoperiod or kept under the existing photoperiod. Hypocotyl measurements were then taken on day 5 and day 7 to understand the immediate and long-term impact of the shift, respectively. We transferred seedlings on day 3 as hypocotyl development in de-etiolated Arabidopsis seedlings primarily occurs between three- and four-days post-germination [6]. Supporting this, we found minimal difference in median hypocotyl length of Ws-2 seedlings grown under SD and LD on day 3 (Figure 1B). To compare the relative amount of photoperiodic memory between Arabidopsis ecotypes and mutants with different hypocotyl lengths, we implemented a photoperiodic memory index

(PMI, Figure 1C). The PMI scales the hypocotyl length relative to the median hypocotyl length of growth under LD and SD conditions. Thus, seedlings with a PMI closer to 1 have a hypocotyl length similar to those grown under constant SD, while a score closer to 0 indicates development similar to that of constant LD.

Arabidopsis seedlings display photoperiodic memory

We firstly analyzed the photoperiodic memory of wild-type Arabidopsis Ws-2 seedlings. As discussed above, Ws-2 seedlings were exposed to the photoperiodic shift on day 3 (Figure 2A). By day 5, hypocotyl development in the Ws-2 seedlings that underwent either photoperiod shift had a PMI of ~0.45 (Figure 2B, Supplementary Figure 1), indicating that exposure to the initial photoperiod does influence hypocotyl development. By day 7, hypocotyl development in the seedlings that underwent the photoperiod shift had diverged from each other and were more closely resembling those under constant conditions (Figure 2C). However, for neither photoperiod shift did hypocotyl elongation mirror that of seedlings grown under a constant photoperiod (Figure 2C). Together, these results suggest that hypocotyl development displays evidence of a lasting photoperiodic memory.

Next, we investigated whether other Arabidopsis ecotypes also displayed photoperiodic memory and the heterogeneity in response between these ecotypes. Ecotypes were picked to cover a range of latitudes from the equator to northernly latitudes (Supplementary Table 1). For all ecotypes, hypocotyl elongation again displayed evidence of photoperiodic memory and this memory continued to persist on day 7 (Figure 2B-C, Supplementary Figure 1). However, for the Sha, Cvi and Bay-0 ecotypes the memory of the initial photoperiod was weaker than Ws-2 for both photoperiod shifts. We also observed that certain ecotypes displayed stronger memory of a particular photoperiod shift. For example, Tanzania (Tnz) had a stronger memory of the LD-SD than SD-LD transitions on day 5, while Sapporo (Sap) displayed the opposite behavior (Figure 2B). However, neither effect persisted after an additional two days in the final photoperiod (Figure 2C). Importantly, for all ecotypes tested except Ws-2, there was a difference in hypocotyl length between the different photoperiod shifts on day 5 even though the seedlings were exposed to the same amount of total light (Supplementary Figure 2-3). Therefore, it is the order of the photoperiod exposure that is important in determining hypocotyl elongation.

phyB and ELF3 regulate the rate that Ws-2 responds to changes in day length

To understand the genetic pathways underpinning the response to the photoperiodic shifts, we characterized different mutants in the Ws-2 ecotype background (wild type, WT), as this ecotype had the strongest photoperiodic memory (Figure 2). We firstly focused on phyB and ELF3 as they

are key regulators of hypocotyl elongation [4, 5]. On day 5, the *elf3* mutant had reduced photoperiodic memory of both photoperiod shifts relative to Ws-2 (Figure 2D, Supplementary Figure 4-5). On day 7, hypocotyl elongation in the *elf3* mutant remained more sensitive to the SD-LD shift but had a similar response to WT for the LD-SD shift (Figure 2E). For the *phyB* mutant, seedlings phenocopied the WT response to the LD-SD on day 5 but then displayed reduced growth by day 7 (Figure 2D-E). Under the SD-LD shift, *phyB* mutants had a similar PMI to those kept under constant LD (Figure 2D), indicating a weak memory of the initial SD photoperiod. This phenotype became further enhanced by day 7, with *phyB* mutants moved from SD-LD now shorter than those kept under continuous LD (Figure 2E). We also analyzed the *elf3/phyB* mutant phenotype to understand the genetic relationship between ELF3 and phyB. For the LD-SD shift, the *elf3/phyB* mutant phenocopied the WT response at both timepoints (Figure 2D-E). Similarly, for the SD-LD shift the *elf3/phyB* mutant had a similar response to WT at the first timepoint (Figure 2D). However, at the second timepoint the *elf3/phyB* mutant had reduced photoperiodic memory than WT (Figure 2E). Together, our results highlight a complex requirement of phyB and ELF3 in regulating photoperiodic memory: ELF3 is necessary to regulate a plant's initial sensitivity to changes in the photoperiod, while phyB prevents over-compensation for the SD-LD shift and sensitizes plants to the shift to SD.

The impact of photoperiodic memory is dependent on developmental age

Hypocotyl elongation is dependent on the accumulation of PIFs at specific time of day. Maximal hypocotyl elongation occurs under SD photoperiods as PIF accumulation coincides with the late evening, where PIF activity displays minimal inhibition [3, 7]. This led us to investigate how the dynamics of hypocotyl elongation changes across time in seedlings that underwent the photoperiod shift. For this experiment, seeds were stratified in water rather than on the surface of the agar-media for 3 days. This small change in the protocol delayed the onset of hypocotyl emergence until day 3, the point at which the photoperiod shift initiates. Thus, the perception of the initial photoperiod under these conditions occurred exclusively in the germinating seed. This allowed us to subsequently investigate how photoperiodic perception in seeds influences seedling development alongside the effects of the photoperiod shifts on the timing of hypocotyl elongation.

Intriguingly, WT seedlings whose germinating seeds were exposed to LD, but then shifted to SD had extremely rapid hypocotyl elongation, compared to all other conditions (Figure 3A). The timing of growth in seeds that were shifted from LD-SD was consistent with those grown under constant SD conditions (Figure 3B). However, the maximal growth rate in the seeds that were shifted from LD-SD was much higher on the first night and remained elevated on the second night.

109 Thus, the shift from LD-SD caused a temporary acceleration of growth. For the SD-LD shift, Ws-2
110 displayed a less pronounced memory of the initial SD exposure, with overall hypocotyl elongation
111 (Figure 3A) and the timing of growth (Figure 3B) closely mirroring seedlings that were only
112 grown under constant LD. In summary, Ws-2 seeds display photoperiodic memory of prior LD
113 exposure, and this results in sustained levels of increased hypocotyl elongation when shifted to
114 SD.
115
116 As ELF3 and phyB were required for photoperiodic memory in seedlings, we investigated
117 whether they contributed to photoperiodic memory in seeds. phyB is functional in seeds [8, 9]
118 and the circadian clock is also active in imbibed seeds [10]. The role of ELF3 in seeds remains to
119 be determined. As in WT, the *elf3, phyB* and *elf3/phyB* mutants' overall growth and the timing of
120 growth showed weak memory of the SD-LD shift (Figure 3A-B). For the LD-SD shift, the *elf3*
121 mutant did not display enhanced growth on the first night (Figure 3B). Instead, the enhanced
122 growth was delayed until the second night. Furthermore, the peak timing of this growth was
123 shifted from late evening to dusk, where ELF3 functions within the evening complex to repress
124 *PIF4/5* expression [11]. As with WT, *elf3* mutants displayed two evenings of accelerated growth
125 following the LD-SD shift before the rate of hypocotyl elongation became more consistent with
126 growth under constant SD (Figure 3B). In the *phyB* mutant, there was no evidence of accelerated
127 growth following from the shift from LD-SD. Instead, growth displayed two smaller peaks at dusk
128 and in the late evening. These two smaller peaks of growth likely compensate for the absence of
129 one predominant period of growth. The *elf3/phyB* mutant displayed similar phenotypes to the
130 respective single mutants for the LD-SD shift, with both a delay in the adjustment to the new
131 photoperiod and an absence of a major peak of growth (Figure 3B). Thus, phyB and ELF3
132 seemingly work independently to control the acceleration of growth and adjustment to the new
133 photoperiod, respectively, following the LD-SD shift.
134
135 **Circadian clocks adapt to photoperiod shifts quickly in Arabidopsis seedlings**
136 Although our data suggests that seeds and seedlings have a memory of the prior photoperiod, it
137 is unclear how this photoperiodic information is stored. One possible mechanism is through the
138 circadian clock. The circadian clock has a critical role in regulating photoperiodic responses in
139 plants [1-3]. Furthermore, the circadian clock is active in imbibed seeds [10] and the expression
140 of *PIF4* and *PIF5* display photoperiod-dependent changes in the phase of their expression [3].
141 Thus, we hypothesized that the circadian clock may function as a repository for photoperiodic
142 information.
143

144 To test this possibility, we analyzed the circadian waveform of the *CCR2::LUC* reporter in the Ws-
145 2 background. Here, seedlings were entrained for ten days under SD (8/16 light/dark) and then
146 shifted to LD for three days. As a control, seedlings were entrained and then kept under SD or LD
147 for the length of the experiment. For seedlings grown under either constant SD or LD conditions,
148 *CCR2::LUC* was phased to the early evening of each respective photoperiod as reported previously
149 [12, 13]. In seedlings that underwent the photoperiod shift, the phase of *CCR2::LUC* was initially
150 between the phase of *CCR2::LUC* in either constant SD or constant LD seedlings (Figure 4A).
151 However, by the second day post-shift, the phase of the *CCR2::LUC* reporter became aligned with
152 seedlings that were grown under constant LD. As hypocotyl elongation displayed memory of the
153 photoperiod information for at least four days post-shift (Figure 2-3), it is unlikely photoperiodic
154 information stored by the circadian clock can sufficiently explain the developmental responses
155 we have observed.
156
157 Although it is unlikely that circadian clock provides photoperiodic memory, we were interested
158 in understanding the heterogeneity of the response to the SD-LD shift. To investigate this, we
159 visualized the individual responses of each plant that underwent the shift using a functional
160 Principle Component Analysis (PCA) (see methods). We included three points for each individual
161 plant measured from the day before the shift, the day of the shift, and the day after the shift. Each
162 point represents the shape of the circadian rhythm across the respective day. This plot can be
163 interpreted in the same way as a traditional PCA plot, so days with similarly phased circadian
164 rhythms should group together. We found that there were individual plants that had rhythms that
165 resembled those under LD prior to the SD to LD shift and conversely there were individual plants
166 that had rhythms resembling SD plants two days after the shift (Figure 4B). However, this was a
167 very small proportion of the total plants evaluated. Therefore, the re-adjustment of circadian
168 phase following the photoperiod shift is very robust and uniform. In summary, hypocotyl
169 photoperiodic memory is unlikely to be directly controlled by the circadian clock.
170
171 **Other Brassicaceae display strong photoperiodic memory.**
172 Next, we investigated whether photoperiodic memory was present in other plants. Here, we
173 focused on microgreens that are grown in vertical farms as the hypocotyl is the primary
174 commercial product [14]. Microgreens grown under LD photoperiods have enhanced nutritional
175 quality, but the longer photoperiods are associated with higher operational energy costs.
176 Alongside reducing energy consumption, shorter photoperiods will also induce hypocotyl
177 elongation, increasing the quantity of yield. We hypothesized that photoperiodic memory may
178 enable us to combine the benefit of growth under both photoperiods. To investigate this
179 possibility, we firstly focused on kale and radish crops that are grown as microgreens within

180 vertical farms. As with Arabidopsis, kale and radish displayed evidence of photoperiodic memory
181 (Figure 4C, Supplementary Figure 6). However, all three cultivars that were tested displayed
182 stronger photoperiodic memory than Arabidopsis. Seedlings shifted from SD-LD had a PMI closer
183 to those grown under constant SD, while those shifted from LD-SD had a PMI similar to those
184 grown under constant LD. Moreover, the plants that experienced a SD to LD shift were also less
185 etiolated and had greener coloration, which is an agriculturally advantageous trait (Figure 4C).
186 These results suggest that photoperiod shifts may have immediate uses in optimizing growth
187 conditions in vertical farms.
188
189 **Concluding statement**
190 In summary, our work has a previously unknown mechanism of photoperiodic memory that
191 controls hypocotyl development. Distinct pathways seem to operate to control the response to
192 different directions of photoperiodic shifts, and the impact of the memory is dependent on the
193 developmental age of the plant. The genetic pathway that regulates photoperiodic memory is
194 unclear, but it seems to occur independently of transcriptional circadian rhythms. Photoperiodic
195 memory may have immediate direct agricultural implications by allowing the optimization of
196 nutritional quality, yield, and operational costs of vertical farms. It will be important to test the
197 presence of photoperiodic memory outside of Brassicaceae to understand the wider potential
198 benefits of photoperiodic memory in other agricultural settings.
199
200 **Methods**
201 Plant lines and husbandry.
202 The following *Arabidopsis thaliana* ecotypes were used in this work: Bay-0, Cape Verde Island
203 (Cvi), Sapporo (Sap), Shakdara (Sha), Tanzania-1 (Tnz-1) and Wassilewskija-2 (Ws-2). All
204 ecotypes harbored the *CCR2::LUC* reporter gene. Bay-0 *CCR2::LUC*, Cvi *CCR2::LUC*, Sha *CCR2::LUC*
205 and Ws-2 *CCR2::LUC* have been described previously [15-17]. For the Sap and Tnz *CCR2::LUC*
206 lines, the respective parent background were transformed with the *CCR2::LUC* reporter by floral
207 dip [18]. A luminesce transgenic plant was then identified and backcrossed to the respective
208 parental line. This backcrossed transgenic was then self-fertilized before a homozygous, single
209 transgene segregant was identified and bulked in the following generation. The following
210 Arabidopsis mutants in the Ws-2 background were also used: *elf3-4 CCR2::LUC*, *phyB-10*
211 *CCR2::LUC*, *elf3-4/phyB-10 CCR2::LUC*. These mutants have been previously described in earlier
212 work [4, 19, 20]. Prior to experiments, all lines were propagated on soil in environmentally
213 controlled growth chambers with a long-day photoperiod (16/8 L/D) at a light intensity of 100
214 $\mu mol/m^{-2}/s^{-1}$ and a set temperature of 22°C.
215

216 Hypocotyl measurements.

217 For the collection of data presented in figure 1, figure 2 and supplementary figure 1-4, all seeds
218 were surface sterilized before being plated onto 1x Murashige and Skoog (MS) media with 1.5%
219 w/v phytoagar (Duchefa), 1% w/v sucrose (Sigma) and 0.5 g/L MES (Sigma). Seeds were then
220 stratified for 48-96 hours. After stratification, germination was induced by exposure to 75
221 $\mu mol/m^{-2}/s^{-1}$ of white light for 24 hours and a constant temperature of 19.5°C. After 24 hours,
222 germinating seeds were provided photoperiod information. They were either grown under short-
223 days (SD, 6/18) or long-days (LD, 16/8) photoperiods with a constant temperature of 19.5°C and
224 a light intensity of 75 $\mu mol/m^{-2}/s^{-1}$. After 48 hours, the photoperiod shifts were initiated.
225 Seedlings were either kept under the initial photoperiod as a control or transferred to the
226 reciprocal photoperiod. All photoperiod shifts occurred at ZT6, before lights off for the SD growth
227 conditions. Measurements were taken on day 5 (timepoint 1) or day 7 (timepoint 2) at ZT6. All
228 experiments were repeated twice with a similar result observed across the two experimental
229 repeats. The presented data is a combination of the two experimental repeats, with each
230 individual experiment including at least fifteen seedlings. Hypocotyl images were measured using
231 imageJ [21]. For figures 1 and 2, hypocotyl measurements were scaled so that the median LD
232 hypocotyl length was 0 and the median SD hypocotyl length was 1, using the formula: *Scaled*
233 *length = (length – median length LD)/(median length SD – median length LD).* Adjusted p-values
234 were calculated using TukeyHSD tests. We have included all statistical and raw hypocotyl
235 measurements as a supplementary dataset (Supplementary File).

236

237 Luciferase assay.

238 Arabidopsis Ws-2 *CCR2::LUC* WT seeds were surface sterilized and plated on 1x MS medium
239 containing 3% w/v sucrose (Sigma), 1.5% w/v phytoagar (Duchefa), 0.5 g/L MES (Sigma) and 15
240 µg/ml Hygromycin-B. After 5 days of stratification at 4°C, seeds were transferred to the specified
241 photoperiod for 6 days. For all photoperiods, a constant temperature of 20°C was used and a light
242 intensity of between 80 - 100 $\mu mol/m^{-2}/s^{-1}$. On day 6, seedlings were transferred into a 96 well
243 plate containing the same media as described above but additionally 15 µl of 1 mM Luciferin.
244 Plates were then placed back in the growth cabinet until they were then transferred to the
245 TOPCOUNT (TC) at dawn on day 7. Plates in the TC were grown under the stated photoperiod
246 with red plus blue light (2.4-3.6 $\mu mol/m^{-2}/s^{-1}$ red light and 0.8-1.4 $\mu mol/m^{-2}/s^{-1}$ blue light) and a
247 constant temperature of 20°C for a further 4 days. For samples undergoing a photoperiod shift,
248 this shift occurred on day 11, exactly 96 hours after being placed in the TC. The fda package in R
249 was used to smooth curves using B-splines and perform functional principal component analysis.

250 Continuous monitoring of hypocotyl elongation.

251 Sterilized Arabidopsis seeds were stratified in darkness at 4°C for 72 hours. To avoid contact of
252 seedlings with the media surface during hypocotyl elongation, two strips were cut and removed
253 from the cultivation medium. Solid *A. thaliana* solution (ATS) nutrient medium [22] with 1% w/v
254 sucrose was used as the cultivation media for these experiments. Seeds were sown in small
255 indentations on the surface of the cut to prevent excessive movement as described previously
256 [23]. Plates were placed vertically at 21°C and constant light (LL, 40 μmol $m^{-2}s^{-1}$) for one day to
257 allow uniform germination of seeds, before being transferred to the initial photoperiod: either LD
258 (16/8 light/dark) or SD (8/16 light/dark) conditions. After two days, plates were transferred to
259 the alternative photoperiod (SD or LD, dawn-aligned), or were kept under the initial photoperiod.
260 The analysis of hypocotyl elongation then started 72 hours after sowing (ZT0). Seedlings were
261 illuminated by two infrared light emitting diodes and were imaged hourly by a Panasonic G5
262 camera modified with a long pass filter (830 nm). To detect minor changes between time points,
263 image stacks were imported as "Image Sequence" in ImageJ. Each seedling ($n \gtrsim 6$) was analyzed
264 separately, and the hypocotyl length was measured using the "Segmented Line" tool, by slightly
265 adjusting the control nodes between time points.
266

267 Hypocotyl Elongation in Microgreens

268 Microgreens (Supplementary Table 2) seeds were sown into trays containing a compost mix
269 comprised of equal parts F2+S (Levington), coir and vermiculite supplemented with 0.7 g/L
270 osmocote fertiliser. Seeds were sown approximately 1cm below the surface of the soil.
271 Microgreens were then grown under either a long-day (16/8) or short-day photoperiod (8/16)
272 photoperiod with a constant temperature of 19°C, 60% humidity and 70 μmol/m^{-2}/s^{-1} of light.
273 Trays were inspected daily to determine when individual hypocotyls had emerged from the soil.
274 Once 50% of the respective microgreen cultivar had a visible hypocotyl, seedlings were grown
275 for three days under the initial photoperiod. This period was determined as the initial
276 photoperiod exposure. After this period, the microgreens were then either switched to the
277 reciprocal photoperiod or kept under the same photoperiod as a control for a further 3 days.
278 Trays were switched at ZT5 to ensure that most of the plants that underwent photoperiod shifts
279 had equal exposure to each photoperiod. Each experiment was carried out three times with 40
280 individual plants imaged per variety per experiment. To image the microgreen hypocotyls, leaves
281 were firstly dissected before the hypocotyls were removed from the soil and laid flat in an Epson
282 scanner. High-resolution scans were then taken. Images were imported into ImageJ for
283 measurement. All imaging took place at ZT5.

284 **Figure Legends.**

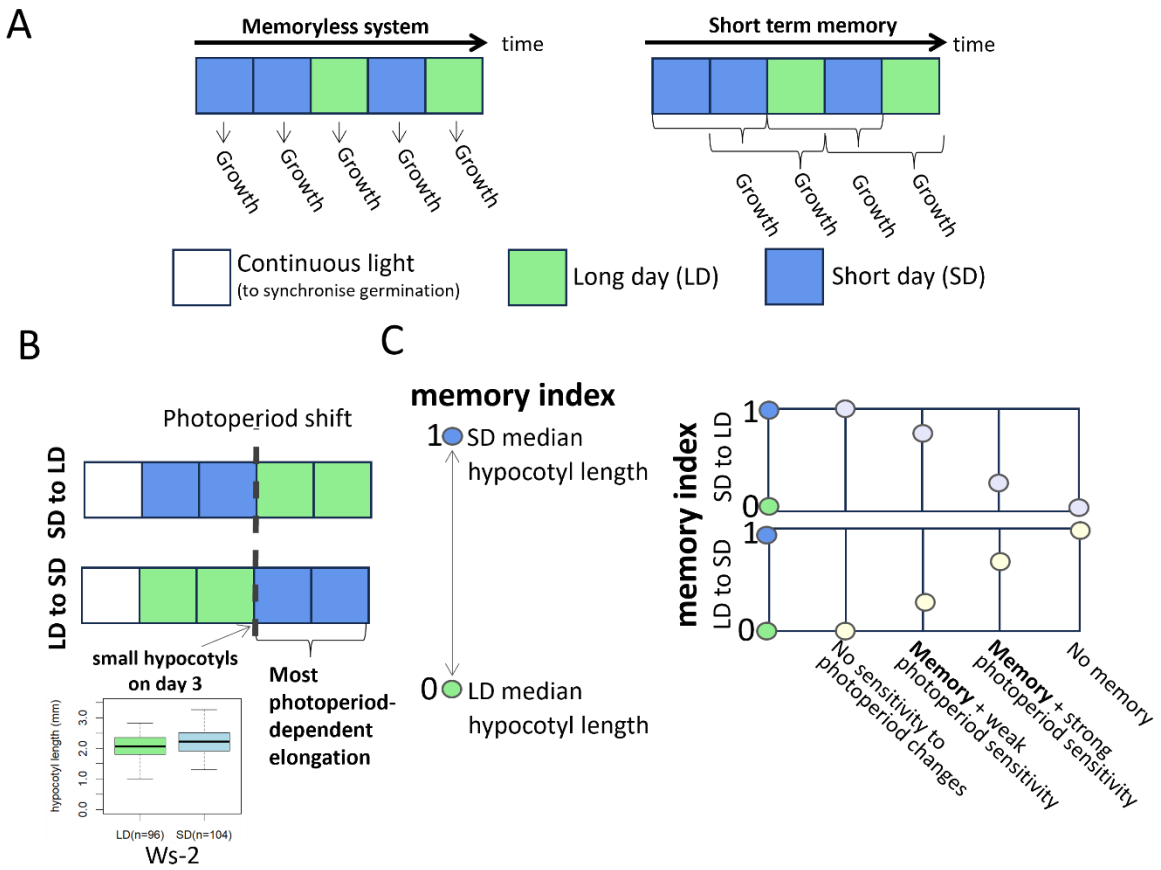

285

286 **Figure 1 –** Designing an assay to test for photoperiodic memory. (A) In the context of this
287 manuscript, we define a 'memory-less system' as one whose growth only depends on the current
288 photoperiod. Conversely, 'memory' refers to growth that also depends on prior environmental
289 conditions. (B) Hypocotyl growth in Arabidopsis seedlings occurs predominantly during the
290 period after the photoperiod shift has occurred. (C) A hypocotyl memory index was used to
291 compare photoperiodic memory and the sensitivity to photoperiodic shifts between ecotypes and
292 mutants that have large magnitudes differences in hypocotyl elongation. Hypocotyl lengths were
293 scaled so that the median hypocotyl length at LD (16/8hr light/dark) is 0 and the median
294 hypocotyl length at SD (8hr/16hr light/dark) is 1.

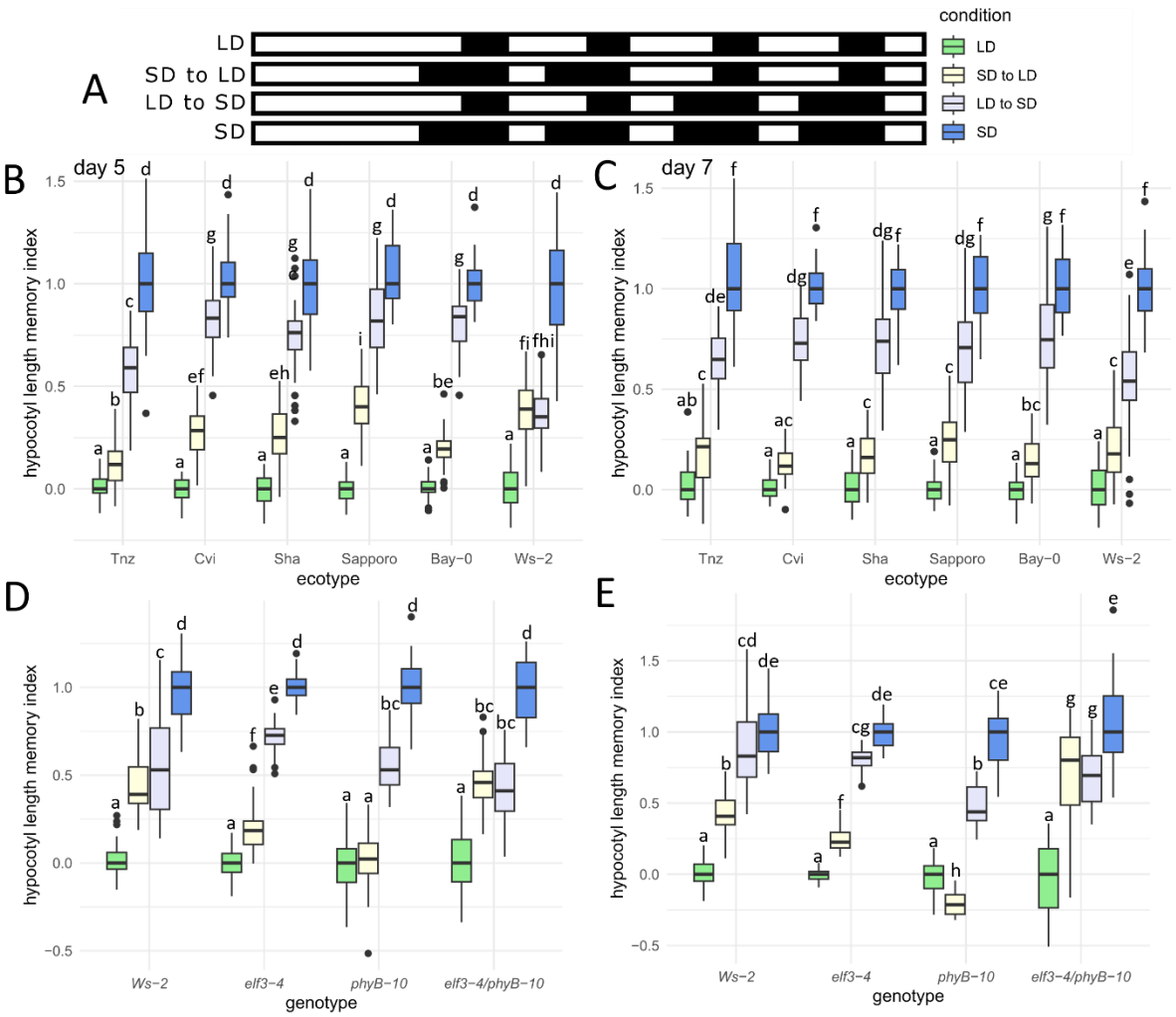

295

296 **Figure 2 –** Hypocotyl development in Arabidopsis displays evidence of photoperiodic memory.
297 (A) Diagram explaining the four different photoperiodic growth conditions, the day phase is
298 white, and the night phase is black. Different Arabidopsis wild type accessions were either
299 measured (B) two or (C) four days after the respective photoperiod shift or were kept under the
300 same photoperiod for the duration of the experiment. Photoperiodic memory response in *elf3-4*,
301 *phyB-10* and *elf3-4/phyB-10* mutants after either (D) two days or (E) four days following the
302 photoperiod shift. Letters signify a significant adjusted p-value of $p < 0.01$, determined by
303 TukeyHSD.

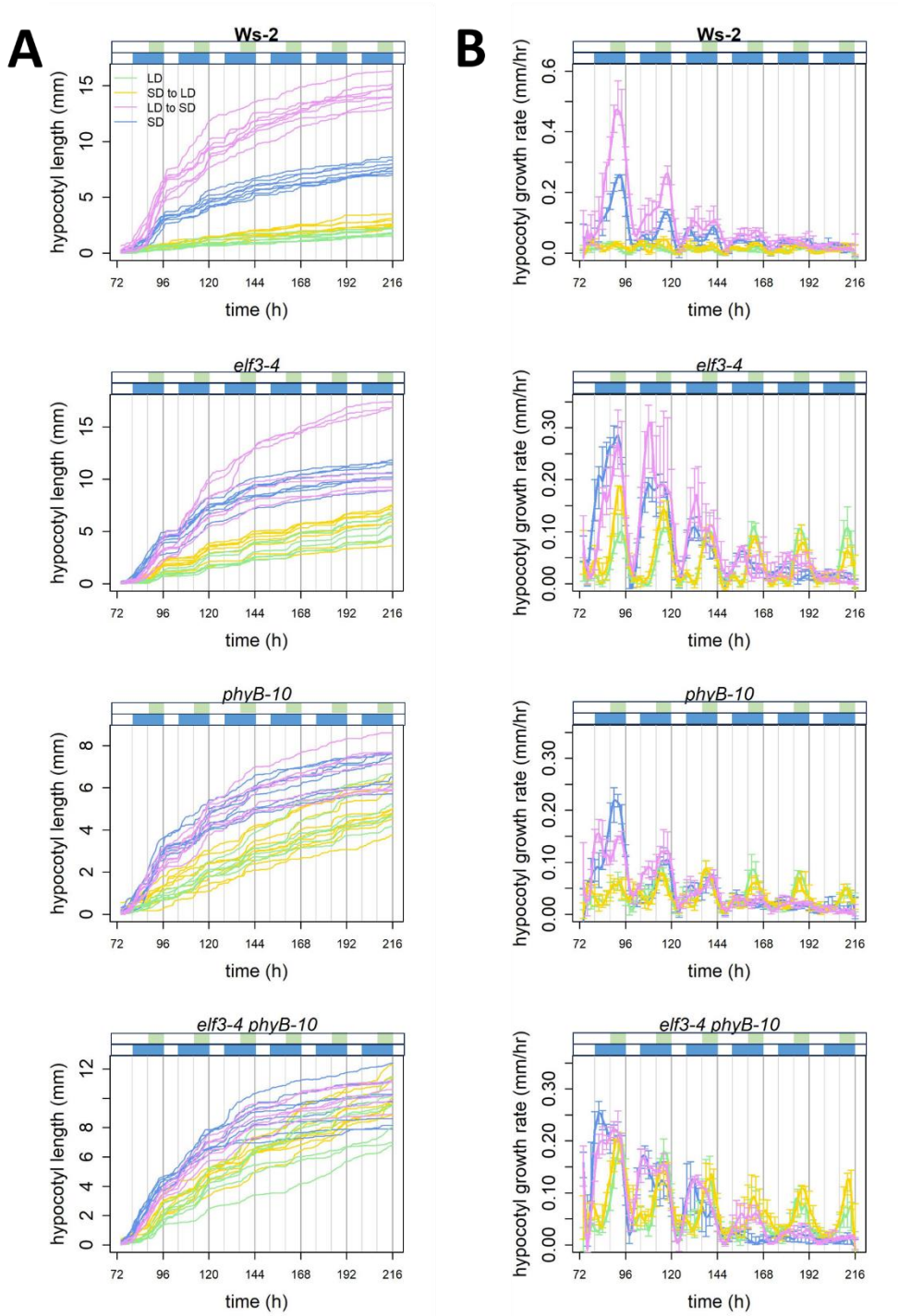

Figure 3 – Photoperiodic memory response is dependent on the developmental age of the plant. (A) Hypocotyl length in Arabidopsis Ws-2 wild-type, *elf3-4*, *phyB-10* and *elf3-4/phyB-10* seedlings under different photoperiodic conditions across time. (B) Hypocotyl growth rate (mm/hr) in the respective genotypes. Highlighted above the plots are the respective photoperiods, long-days in green and short-days in blue. The color boxes highlight the dark phase under the respective photoperiod. All measurements were taken after the photoperiod shift had occurred at ZT72. Note that the seeds germinated later in this experiment than in the experiment depicted in Figure 2, with hypocotyl emergence occurring primarily on day 3.

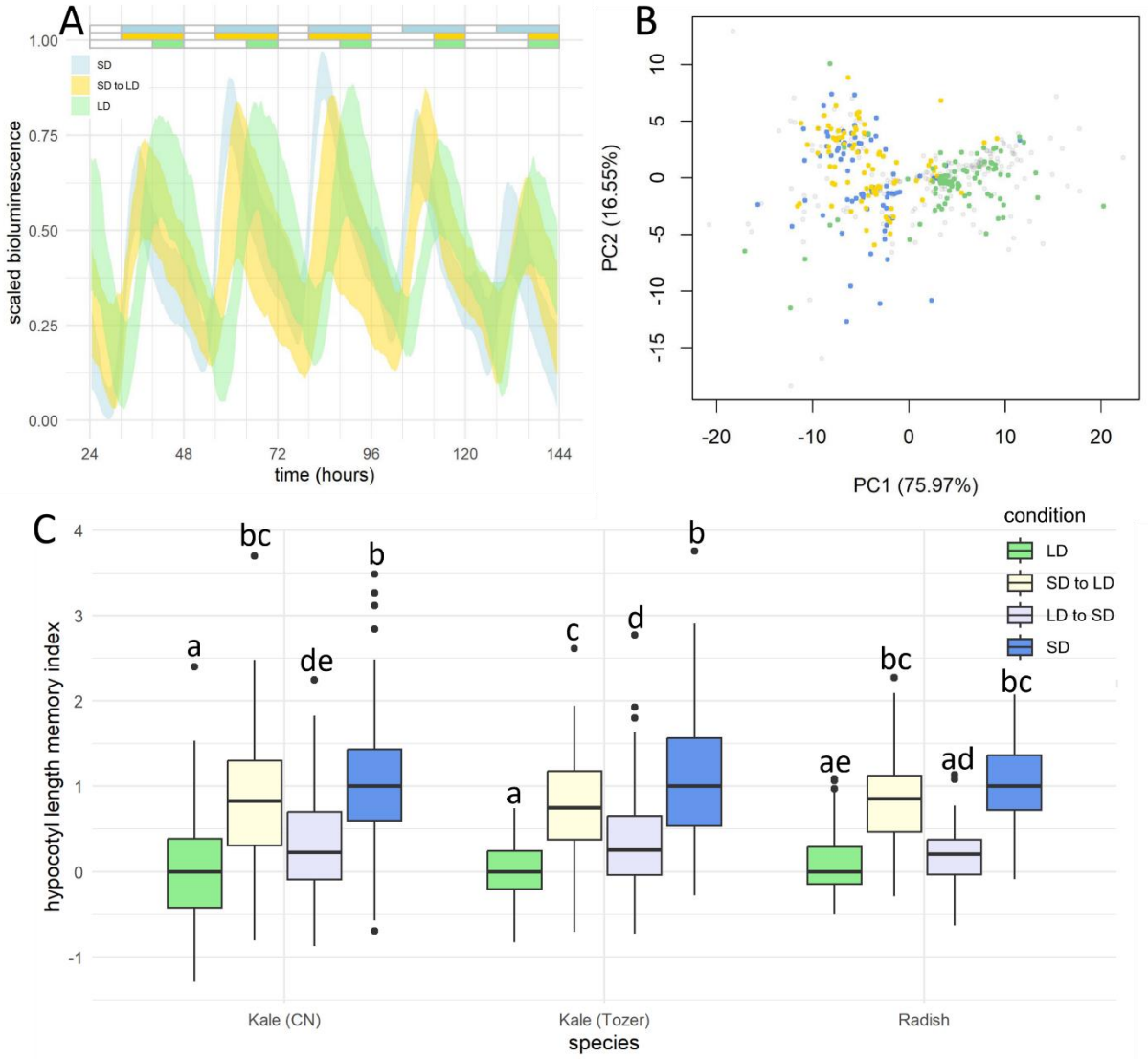

Figure 4 – The circadian clock is unlikely to store photoperiodic memory in Arabidopsis**.** (A) Waveform of *CCR2::LUC* bioluminescence in Ws-2 wild-type seedlings grown under continuous SD (blue) or LD (green) or in seedlings shifted from SD to LD (yellow). (B) A functional PCA (fPCA) plot, where each point represents a different bioluminescence curve for an individual plant, color-coded by their photoperiod condition that plant was exposed to, using a color-scheme consistent with (A). fPCA is interpreted in the same way as a standard PCA, as a projection of data (in this case, coefficients of a complex B-spline function) to a lower dimensional space. (C) Kale (CN seeds), Kale (Tozer seeds) and radish plants used in microgreen agriculture displayed evidence of photoperiodic memory. Letters signify a significant adjusted p-value of $p < 0.01$, determined by TukeyHSD.

Supplementary Figure 1 – Representative scans of seedlings from wild-type Arabidopsis ecotypes used in this work. Images are from day 5, two days after the photoperiod shift. Scale bar is 5 mm.

Supplementary Figure 2 – Hypocotyl length (mm) of wild-type accessions sorted by total light exposure (hours) on day 5. Dark blue is constant SD, purple are seedlings shifted from LD-SD, yellow is seedlings shifted from LD-SD and green is constant LD.

Supplementary Figure 3 - Hypocotyl length (mm) of wild-type accessions sorted by total light exposure (hours) on day 7. Dark blue is constant SD, purple are seedlings shifted from LD-SD, yellow is seedlings shifted from LD-SD and green is constant LD.

Supplementary Figure 4 – Representative scans of seedlings from wild type Arabidopsis Ws-2, *elf3-4*, *phyB-10* and *elf3-4/phyB-10.* Images are from day 5, the first measurement point. Scale bar is 5 mm.

Supplementary Figure 5 - Hypocotyl length (mm) of wild-type Ws-2, *elf3-4*, *phyB-10* and *elf3-4/phyB-10* sorted by total light exposure (hours) on (A) day 5 and (B) day 7. Dark blue is constant SD, purple are seedlings shifted from LD-SD, yellow is seedlings shifted from LD-SD and green is constant LD.

Supplementary Figure 6 – Representative scans of microgreen seedlings. Microgreens are approximately 11 days old at the end of the experiment Scale bar is 15 mm.

Supplementary File – Raw data and statistical tests associated with the figures of this manuscript.

Acknowledgements

We would like to thank Maarten Koornneef for providing the Tnz-1 seeds. We would also like to acknowledge A. L. Tozer Limited for providing us with radish and kale seeds and the York Biology horticulture staff for their assistance and support with this work.

Conflicts of Interest

D.E. and W.C. are currently part of a Better Food for All Innovate UK grant in collaboration with Farm Urban LTD, A.L. Tozer Limited, Vertically Urban Limited, Nutritank Community Interest Company and Alder Hey Living Hospital Limited.

Grant Funding

We would like to acknowledge the following funding sources: the Royal Society (RGS\R2\212345: D.E.), Biotechnology and Biological Sciences Research Council (Responsive Mode) (BB/V006665/1: S.L, K.M., D.E. and S.J.D.), the Biotechnology and Biological Sciences Research Council (White Rose Doctoral Training Partnership) (BB/T007222/1: E.J.R. and G.Y.W.V.), and GenerationResearch (W.C.).

Supplementary Table 1 – Arabidopsis ecotypes used in this work.

Ecotype	Latitude	Longitude	Country
Wassilewskija-2 (Ws-2)	52.3	30.0	Belarus
Tanzania (Tnz)	-2.9	36.2	Tanzania
Bay-0	49.0	11.0	Germany
Shakdara (Sha)	38.4	68.5	Tajikistan
Cape Verde Island (Cvi)	15.1	-23.6	Cape Verde Island
Sapporo (Sap)	43.1	141.3	Japan

Supplementary Table 2 – Microgreen cultivars used in this work

Microgreen	Species	Variety
Kale (Tozer Seeds)	*Brassica oleracea*	Dwarf Green Curled
Kale (CN Seeds)	*Brassica oleracea*	Dwarf Blue
Radish	*Raphanus raphanistrum*	Sangrin

371 **References**

372 1. Song, Y.H., et al., *Photoperiodic flowering: time measurement mechanisms in*
373 *leaves*. Annu Rev Plant Biol, 2015. **66**: p. 441-64.
374 2. Nozue, K., et al., *Rhythmic growth explained by coincidence between internal and*
375 *external cues*. Nature, 2007. **448**(7151): p. 358-61.
376 3. Niwa, Y., T. Yamashino, and T. Mizuno, *The circadian clock regulates the*
377 *photoperiodic response of hypocotyl elongation through a coincidence*
378 *mechanism in Arabidopsis thaliana*. Plant Cell Physiol, 2009. **50**(4): p. 838-54.
379 4. Reed, J.W., et al., *Mutations in the gene for the red/far-red light receptor*
380 *phytochrome B alter cell elongation and physiological responses throughout*
381 *Arabidopsis development*. The Plant Cell, 1993. **5**(2): p. 147-157.
382 5. Zagotta, M.T., et al., *The Arabidopsis ELF3 gene regulates vegetative*
383 *photomorphogenesis and the photoperiodic induction of flowering*. Plant J, 1996.
384 **10**(4): p. 691-702.
385 6. Gendreau, E., et al., *Cellular Basis of Hypocotyl Growth in Arabidopsis thaliana*.
386 Plant Physiology, 1997.
387 7. Leivar, P. and E. Monte, *PIFs: systems integrators in plant development*. Plant
388 Cell, 2014. **26**(1): p. 56-78.
389 8. Lee, K.P., et al., *Spatially and genetically distinct control of seed germination by*
390 *phytochromes A and B*. Genes & Development, 2012. **26**(17): p. 1984-1996.
391 9. Piskurewicz, U., et al., *The Arabidopsis endosperm is a temperature-sensing*
392 *tissue that implements seed thermoinhibition through phyB*. Nature
393 Communications, 2023. **14**(1): p. 1202.
394 10. Zhong, H.H., et al., *Imbibition, but not release from stratification, sets the*
395 *circadian clock in Arabidopsis seedlings*. The Plant Cell, 1998. **10**(12): p. 2005-
396 2017.
397 11. Nusinow, D.A., et al., *The ELF4-ELF3-LUX complex links the circadian clock to*
398 *diurnal control of hypocotyl growth*. Nature, 2011. **475**(7356): p. 398-402.
399 12. Strayer, C., et al., *Cloning of the Arabidopsis Clock Gene TOC1, an Autoregulatory*
400 *Response Regulator Homolog*. Science, 2000. **289**(5480): p. 768-771.
401 13. Schultz, T.F., et al., *A role for LKP2 in the circadian clock of Arabidopsis*. Plant Cell,
402 2001. **13**(12): p. 2659-70.
403 14. Bhaswant, M., et al., *Microgreens-A Comprehensive Review of Bioactive*
404 *Molecules and Health Benefits*. Molecules, 2023. **28**(2).
405 15. Doyle, M.R., et al., *The ELF4 gene controls circadian rhythms and flowering time*
406 *in Arabidopsis thaliana*. Nature, 2002. **419**(6902): p. 74-7.
407 16. Boikoglou, E., et al., *Environmental memory from a circadian oscillator: the*
408 *Arabidopsis thaliana clock differentially integrates perception of photic vs.*
409 *thermal entrainment*. Genetics, 2011. **189**(2): p. 655-64.
410 17. Anwer, M.U., et al., *Natural variation reveals that intracellular distribution of ELF3*
411 *protein is associated with function in the circadian clock*. eLife, 2014. **3**: p.
412 e02206.
413 18. Davis, A.M., et al., *Protocol: Streamlined sub-protocols for floral-dip*
414 *transformation and selection of transformants in Arabidopsis thaliana*. Plant
415 Methods, 2009. **5**: p. 3.
416 19. Hicks, K.A., et al., *Conditional circadian dysfunction of the Arabidopsis early-*
417 *flowering 3 mutant*. Science, 1996. **274**(5288): p. 790-792.

20. Ronald, J., et al., *Cellular localization of Arabidopsis EARLY FLOWERING3 is responsive to light quality*. Plant Physiology, 2022.
21. Schneider, C.A., W.S. Rasband, and K.W. Eliceiri, *NIH Image to ImageJ: 25 years of image analysis*. Nature Methods, 2012. **9**(7): p. 671-675.
22. Lincoln, C., J.H. Britton, and M. Estelle, *Growth and development of the axr1 mutants of Arabidopsis*. Plant Cell, 1990. **2**(11): p. 1071-80.
23. Janitza, P., et al., *A Guide to Quantify Arabidopsis Seedling Thermomorphogenesis at Single Timepoints and by Interval Monitoring*, in *Thermomorphogenesis: Methods and Protocols*, M. Chen, Editor. 2024, Springer US: New York, NY. p. 3-16.